η and η′ in a coupled Schwinger-Dyson and Bethe-Salpeter approach. II. The γ*γ transition form factors

Kekez, Dalibor; Klabučar, Dubravko

η and η' in a coupled Schwinger-Dyson and Bethe-Salpeter approach. II. The $\gamma^*\gamma$ transition form factors

Dalibor Kekez
Rudjer Bošković Institute, P.O. Box 180, 10002 Zagreb, Croatia

Dubravko Klabučar
Department of Physics, Faculty of Science, Zagreb University, P.O. Box 331, 10002 Zagreb, Croatia
(Received 25 September 2001; published 28 January 2002)

The applications of the consistently coupled Schwinger-Dyson and Bethe-Salpeter approach to the η-η' complex are extended to the two-photon transition form factors of η and η' for spacelike transferred momenta. We compare our predictions with experiment and some other theoretical approaches.

DOI: 10.1103/PhysRevD.65.057901 PACS number(s): 11.10.St, 13.40.Gp, 14.40.Aq, 14.40.−n

In Ref. [1], hereafter called paper I, we studied the η-η' complex and its $\gamma\gamma$ decays in a coupled Schwinger-Dyson and Bethe-Salpeter (SD-BS) approach (reviewed recently in, e.g., [2–4]). We obtained the pertinent masses, the pseudoscalar state mixing angle θ, the results for the axial-vector current decay constants of η_8, η_0 and of their physical combinations η and η', the results for the $\gamma\gamma$-decay constants of η_0 and η_8, for the two-photon decay widths of η and η', and for the mixing-independent R ratio constructed from them. On the other hand, the form factors for the transitions $\gamma^*\gamma\to\eta$ and $\gamma^*\gamma\to\eta'$, where γ^* denotes an off-shell photon, were *not* studied in paper I, although Ref. [5] (see also Ref. [6]) addressed the closely related topic of the $\gamma^*\gamma\to\pi^0$ transition form factor. Namely, in that paper the pion was treated *in the chiral (and soft) limit*, which made plausible certain simplifications in the description of the pseudoscalar quark-antiquark ($q\bar{q}$) bound state [see the approximation (2) below], making the calculation a lot easier. Nevertheless, η and η' contain significant $s\bar{s}$ components, which are rather massive. This obviously makes such chiral-limit-based simplifications implausible in a *quantitative* treatment of the $\gamma^*\gamma\to\eta$ and $\gamma^*\gamma\to\eta'$ form factors. Having to refrain therefore from the chiral limit simplifications, while having to deal with the complications due to one off-shell photon, made paper I relegate to a later paper the extension of the η, $\eta'\to\gamma\gamma$ calculations to the off-shell case.

Now, however, we are ready to take up the task of studying the off-shell $\gamma^*\gamma\to\eta,\eta'$ amplitudes and supplement the results of paper I with them, because our subsequent Ref. [7] went beyond the chiral and soft limit approximation when calculating the pion $\gamma^*\gamma$ transition form factor. In other words, it went beyond the approximation where the $q\bar{q}$ bound state pseudoscalar vertex (say, of π^0) of the total momentum p,

$$\Gamma_{\pi^0}(q,p)\equiv\frac{\lambda^3}{\sqrt{2}}\,\mathrm{diag}[\Gamma_{u\bar{u}}(q,p),\Gamma_{d\bar{d}}(q,p),\Gamma_{s\bar{s}}(q,p)], \quad (1)$$

is approximated by its leading $O(p^0)$ piece, which depends only on q, the relative momentum of the constituents:

$$\Gamma_{\pi^0}(q,p)\approx\Gamma_{\pi^0}(q,0)_{m=0}=\gamma_5\lambda^3\frac{B(q^2)_{m=0}}{f_\pi}. \quad (2)$$

Here $\Gamma_{f\bar{f}}$ denotes the $q\bar{q}$ bound-state vertex for the flavor f $(=u,d,s)$, while λ^a denotes the ath $(a=1,...,8)$ Gell-Mann matrix of the flavor SU(3), with λ^3 being the pertinent one for the neutral pion π^0, and $B(q^2)$ the scalar function from the SD solution for the dynamically dressed quark propagator $S(q)=[A(q^2)\not{q}-B(q^2)]^{-1}$. The subscript $m=0$ indicates the case of vanishing *explicit* chiral symmetry breaking. This case is quite close to reality in the case of pions, which are almost massless. Nevertheless, in contradistinction to the SD-BS calculation of the on-shell decay $\pi^0\to\gamma\gamma$, keeping only $O(p^0)$ terms, as in the right-hand side of Eq. (2), turned out to be rather inadequate for calculation of the $\gamma^*\gamma\to\pi^0$ form factors even in the pion case [7,8]. Therefore, Ref. [7] used a *complete* solution for the BS vertex $\Gamma_{\pi^0}(q,p)$ [or equivalently, for the BS amplitude $\chi_{\pi^0}(q,p)\equiv S(q+p/2)\Gamma_{\pi^0}(q,p)S(q-p/2)$], given by the decomposition into four scalar functions $\Gamma_i^{f\bar{f}}(q,p)$ multiplying independent spinor structures, as in Eq. (9) in paper I,

$$\Gamma_{f\bar{f}}(q,p)=\gamma_5\{\Gamma_0^{f\bar{f}}(q,p)+\not{p}\Gamma_1^{f\bar{f}}(q,p)+\not{q}\Gamma_2^{f\bar{f}}(q,p)+[\not{p},\not{q}]\Gamma_3^{f\bar{f}}(q,p)\}. \quad (3)$$

In the isospin limit, which we adopt as an excellent approximation, the $u\bar{u}$ and $d\bar{d}$ bound states have identical BS vertices, $\Gamma_{u\bar{u}}(q,p)=\Gamma_{d\bar{d}}(q,p)$. However, the BS vertex $\Gamma_{s\bar{s}}(q,p)$, pertaining to the much more massive strange quarks, $f=s$, is significantly different [9,10,1].

Using a complete solution (3) in the manner of Ref. [7], but now also for $f=s$, makes us able to calculate adequately the off-shell amplitudes $T_{f\bar{f}}(k^2,k'^2)$ for the transitions from $\gamma^*(k)\gamma^{(*)}(k')$ to $f\bar{f}$ pseudoscalar of momentum $p=k+k'$, where $k^2\neq0$ (and possibly also $k'^2\neq0$). See Eqs. (27) and (24) and (25) in paper I for the definition of $T_{f\bar{f}}(k^2,k'^2)$ and the explicit expression used both for calculating it there for the on-shell case ($k^2=k'^2=0$) and in the present off-shell application. The $\gamma^*\gamma^{(*)}$ transition amplitudes of the physical particles η and η', denoted, respectively, by

$T_\eta(k^2,k'^2)$ and $T_{\eta'}(k^2,k'^2)$, are then obtained as the appropriate mixtures of $T_{f\bar{f}}(k^2,k'^2)$, e.g., as the obvious off-shell generalization of Eqs. (38) and (39) in paper I.

The mixing scheme used in paper I was the octet-singlet one, where η and η' are given through the octet-singlet mixing angle θ and the $SU(3)_f$ octet and singlet isospin zero states η_8 and η_0. They are in turn defined in the $f\bar{f}$ ($f=u,d,s$) basis by

$$|\eta_8\rangle=\frac{1}{\sqrt{6}}(|u\bar{u}\rangle+|d\bar{d}\rangle-2|s\bar{s}\rangle), \tag{4}$$

$$|\eta_0\rangle=\frac{1}{\sqrt{3}}(|u\bar{u}\rangle+|d\bar{d}\rangle+|s\bar{s}\rangle), \tag{5}$$

where it should be noted that the model calculations in paper I and here employ the *broken* $SU(3)_f$ with an s quark realistically more massive than u and d quarks.

In this paper, nevertheless, we opt to use a mixing scheme different from the one in paper I, namely the nonstrange (NS) -strange (S) scheme. In paper I, it was essential to explain the successful reproduction of the Goldstone character of the $SU(3)_f$ octet state η_8 and the non-Goldstone character of the $SU(3)_f$ singlet state η_0, since the $U_A(1)$ anomaly causes $\eta'\to\eta_0$ to remain massive even though $\eta\to\eta_8$ becomes massless when the chiral limit is taken for all three flavors, m_u, m_d, $m_s\to 0$. The important role of η_8 and η_0, Eqs. (4) and (5), in the discussions in paper I made the octet-singlet mixing scheme the most convenient one to use there. Here, however, it is somewhat more convenient to work in the NS-S basis $|\eta_{\rm NS}\rangle$ and $|\eta_{\rm S}\rangle$, where

$$|\eta_{\rm NS}\rangle=\frac{1}{\sqrt{2}}(|u\bar{u}\rangle+|d\bar{d}\rangle)=\frac{1}{\sqrt{3}}|\eta_8\rangle+\sqrt{\tfrac{2}{3}}|\eta_0\rangle, \tag{6}$$

$$|\eta_{\rm S}\rangle=|s\bar{s}\rangle=-\sqrt{\tfrac{2}{3}}|\eta_8\rangle+\frac{1}{\sqrt{3}}|\eta_0\rangle, \tag{7}$$

and where the NS-S mixing relations are

$$|\eta\rangle=\cos\phi|\eta_{\rm NS}\rangle-\sin\phi|\eta_{\rm S}\rangle, \tag{8a}$$

$$|\eta'\rangle=\sin\phi|\eta_{\rm NS}\rangle+\cos\phi|\eta_{\rm S}\rangle. \tag{8b}$$

The NS-S state mixing angle ϕ is related to the singlet-octet state mixing angle θ as $\phi=\theta+\arctan\sqrt{2}=\theta+54.74°$. The NS-S mixing basis is more suitable for some quark model considerations. In particular, in the case of our η_8 and η_0, we again point out that Eqs. (4) and (5) do not presently define the octet and singlet states of the exact SU(3) flavor symmetry, but rather the $SU(3)_f$-inspired *effective* octet and singlet states, since $|u\bar{u}\rangle$ and $|d\bar{d}\rangle$ are practically chiral states as opposed to a significantly heavier $|s\bar{s}\rangle$. When the symmetry between the NS and S sectors is broken like this, the NS-S mixing basis is more natural in practice. For example, if M_P denotes the mass of the meson P and $\alpha_{\rm em}$ the electromagnetic fine-structure constant, the expressions for the η and $\eta'\to\gamma\gamma$ decay widths in this basis become

$$W(\eta\to\gamma\gamma)=\frac{\alpha_{\rm em}^2}{32\pi^3}\frac{M_\eta^3}{9f_\pi^2}\left[\frac{5}{\sqrt{2}}\frac{f_\pi}{\bar{f}_\pi}\cos\phi-\frac{f_\pi}{\bar{f}_{s\bar{s}}}\sin\phi\right]^2, \tag{9}$$

$$W(\eta'\to\gamma\gamma)=\frac{\alpha_{\rm em}^2}{32\pi^3}\frac{M_{\eta'}^3}{9f_\pi^2}\left[\frac{5}{\sqrt{2}}\frac{f_\pi}{\bar{f}_\pi}\sin\phi+\frac{f_\pi}{\bar{f}_{s\bar{s}}}\cos\phi\right]^2, \tag{10}$$

instead of Eqs. (40) and (41) in paper I. That is, instead of using the $\gamma\gamma$-decay constants $\bar{f}_{\eta_8}$ and $\bar{f}_{\eta_0}$ [see Eqs. (29) and (30) in paper I], one writes the $\gamma\gamma$-decay amplitudes through analogously defined $s\bar{s}$ two-photon decay constant $\bar{f}_{s\bar{s}}$ and the pionic $\gamma\gamma$-decay constant $\bar{f}_\pi$ ($\approx f_\pi$). This NS-S decomposition is more natural for the following reasons. The $\eta_{\rm NS}\to\gamma\gamma$ amplitude, $T_{\eta_{\rm NS}}(0,0)=(1/\sqrt{2})[T_{u\bar{u}}(0,0)+T_{d\bar{d}}(0,0)]=(5/3)T_{\pi^0}(0,0)$, is quite close to its chiral limit value fixed by the QED axial anomaly [see Eqs. (26) and (28) in paper I] since $\bar{f}_\pi$ is approximated well by the usual leptonic (axial-current) decay constant f_π, while $T_{\eta_{\rm S}}(0,0)=T_{s\bar{s}}(0,0)$ is noticeably farther from the chiral limit value. However, at least $\bar{f}_{s\bar{s}}\approx f_{s\bar{s}}$ is ensured through the Goldberger-Trieman (GT) relation (which is a natural result in the SD-BS approach). In contradistinction to that, for the decay constants appearing in the octet-singlet decomposition, $\bar{f}_{\eta_8}<f_{\eta_8}$ rather generally [1,11] in the quark-based approaches.

Another advantage of the $\eta_{\rm NS}$-$\eta_{\rm S}$ state mixing angle ϕ is that one then easily notes the consistency of our (in paper I and Refs. [11–13]) preferred mixing angle $\phi=42°$ with the value of ϕ obtained in the recent thorough analysis of Feldmann, Kroll, and Stech (FKS) [14,15]. For reasons related to this, the NS-S mixing basis also offers the most straightforward way to show the consistency of our procedures and the corresponding results obtained using just one (θ or ϕ) state mixing angle with the two-mixing-angle scheme [16,17], which is defined with respect to the mixing of the decay constants. This is explained in detail in Ref. [11], which improved the analysis of mixing in the η-η' complex over that performed in paper I, only to confirm[1] the preferred value of the state mixing angle found already in paper I, namely $\phi=42°$ (or equivalently, $\theta=-12.7°$). This is practically [11] the same as the result of the "FKS scheme and theory" [14,15,18], and in agreement with data. We thus use this mixing angle value in

$$T_\eta(k^2,k'^2)=\cos\phi T_{\eta_{\rm NS}}(k^2,k'^2)-\sin\phi T_{\eta_{\rm S}}(k^2,k'^2), \tag{11}$$

$$T_{\eta'}(k^2,k'^2)=\sin\phi T_{\eta_{\rm NS}}(k^2,k'^2)+\cos\phi T_{\eta_{\rm S}}(k^2,k'^2). \tag{12}$$

[1]See also our shorter Ref. [12].

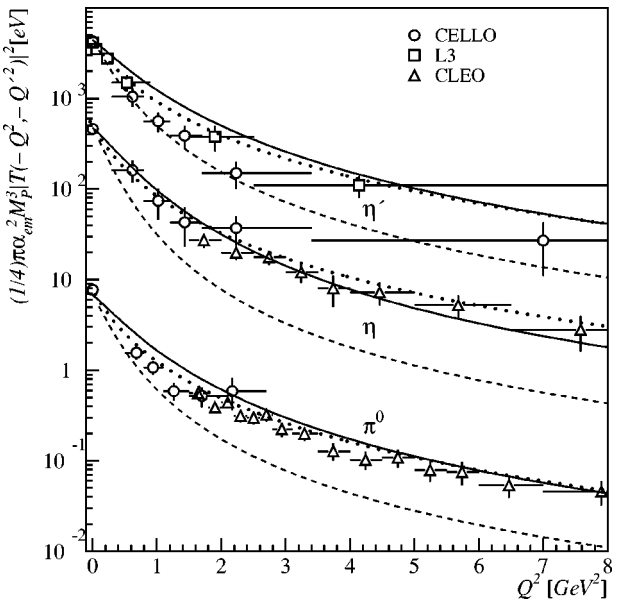

FIG. 1. The Q^2 dependence of various results for the form factors of $P=\eta',\eta,\pi^0$. The curves are obtained through Eq. (13) employing the empirical meson masses, $M_{\eta'}=0.958$ GeV, $M_{\eta}=0.547$ GeV, and $M_{\pi^0}=0.135$ GeV [34]. In the $Q'^2=0$ case, for which we plot data from CELLO [19] (circles), CLEO [23] (triangles), and L3 [24] (squares), the solid curves correspond to our numerically obtained model $\gamma^*\gamma$ transition form factors and the dotted curves correspond to the BL ones. The dashed curves correspond to our $\gamma^*\gamma^*$ model form factors, but for the symmetric case $Q'^2=Q^2$.

These amplitudes are the two-photon transition form factors of η and η'. In Fig. 1, we follow the CELLO collaboration [19] in presenting results on the form factors in terms of the convenient combination

$$\frac{\pi\alpha_{\rm em}^2 M_P^3}{4}|T_P(k^2,k'^2)|^2 \quad (P=\pi^0,\eta,\eta'). \tag{13}$$

Its on-shell limit $k^2=k'^2=0$ returns the η, $\eta'\to\gamma\gamma$ widths (9) and (10) already studied in paper I. In the present paper, we evaluate the amplitudes (11) and (12) in the cases in which one or both photons are off-shell and spacelike, $k^2=-Q^2<0$, $k'^2=-Q^2\leqslant 0$.

Since this paper is the extension of paper I, here we use the same SD-BS model [9,10], model parameters, and solutions for the dressed quark propagators and the corresponding quark-antiquark bound states as in paper I. The incorporation of the quark-photon interactions is also the same as adopted there through the scheme of a generalized impulse approximation, where all propagators, bound-state vertices, and quark-photon vertices are dressed. (This impulse approximation in the present application is illustrated by the pseudoscalar-photon-photon triangle graph in Fig. 1 of paper I.) This is necessary for reproducing exactly and analytically anomalous $\gamma\gamma$ (on-shell) amplitudes[2] in the chiral limit, and requires the usage of a dressed quark-photon vertex satisfying the vector Ward-Takahashi identity. The Ball-Chiu (BC) [22] vertex is used in paper I, and thus also here. The off-shell amplitudes

$$T_{\eta_{\rm NS}}(-Q^2,-Q'^2)=\frac{1}{\sqrt{2}}[T_{u\bar{u}}(-Q^2,-Q'^2)+T_{d\bar{d}}(-Q^2,-Q'^2)]=\tfrac{5}{3}T_{\pi^0}(-Q^2,-Q'^2) \tag{14}$$

(obtained by working, as in paper I, in the isospin limit) and

$$T_{\eta_{\rm S}}(-Q^2,-Q'^2)=T_{s\bar{s}}(-Q^2,-Q'^2) \tag{15}$$

are calculated numerically in the same way as it was done for the pion in Ref. [7], also still keeping the approximation used there, which consists in discarding the second and higher derivatives in the momentum expansions.

The results on the η', η, and π^0 transition form factors are presented in Fig. 1 in the spacelike momentum range $0<Q^2<8$ GeV^2, along with the experimental data [19,23,24]. There are three sets of three theoretical curves each. The highest of these triplets pertains to η', the middle one to η, and the lowest one to π^0. The same holds for the three distinct groups of data.

All of the displayed data points [19,23,24], as well as the solid and dotted curves in each of the curve triplets, pertain to the $\gamma^*\gamma$ case of one photon of spacelike virtuality and one real photon, $Q^2>0$ and $Q'^2=0$. The solid curves in Fig. 1 represent our η', η, and π^0 model form factors (13), obtained through Eqs. (11)–(13) with our preferred $\phi=42°$.

Note that all model input was fixed in Ref. [10] and paper I, so that our transition form factors are pure predictions. The agreement with experiment is thus relatively good, considering the absence of any additional model fitting in this paper. The main deficiency in the description of the data is that our predictions are too high in the intermediate range of transferred momenta, $0.5\,\text{GeV}^2<Q^2<2\,\text{GeV}^2$, at least for η' and π^0.

In Fig. 1, we also plot (by dotted curves) the η', η, and π^0 form factors (13) stemming from the Brodsky-Lepage (BL) *Ansatz* $T_P^{\rm BL}(-Q^2,0)$ for $P=\pi^0$, $\eta_{\rm NS}$, $\eta_{\rm S}$ [25]. We do this to compare in a brief and compact, albeit very rough way, our results with the predictions of Abelian axial anomaly, vector meson dominance (VMD), and perturbative QCD (PQCD) in their regimes of validity. Namely, this *Ansatz* is adjusted so that it agrees with the axial anomaly predictions at $Q^2=0$ [e.g., $T_{\pi^0}(0,0)=1/4\pi^2 f_\pi$], while for large Q^2 it tends to the behavior $\propto 1/Q^2$ predicted by PQCD [25]. Also, due to $8\pi^2 f_\pi^2\approx m_\rho^2\approx m_\omega^2$ and $8\pi^2 f_{\eta_{\rm S}}^2\approx m_\phi^2$, the BL *Ansatz* is not very different from VMD, since their corresponding residues also agree approximately [26]. The BL *Ansatz* was shown to work well not only for $P=\pi^0$, but also $P=\eta,\eta'$ [26]. In the NS-S basis, it is given by

[2]But also others, notably $\gamma\pi^+\to\pi^+\pi^0$; see Refs. [20], [21].

$$T_P^{\mathrm{BL}}(-Q^2,0)=\frac{N_c C_P 2\sqrt{2} f_P}{Q^2}\,\frac{1}{1+\dfrac{8\pi^2 f_P^2}{Q^2}} \quad (P=\pi^0,\eta_{\mathrm{NS}},\eta_{\mathrm{S}}), \tag{16}$$

where $N_c=3$ and the flavor-charge factors are $C_{\pi^0}=1/3\sqrt{2}$, $C_{\eta_{\mathrm{NS}}}=5/9\sqrt{2}$, and $C_{\eta_{\mathrm{S}}}=1/9$. The dotted curves stem from the BL *Ansatze* (16) for the case named ''FKS scheme and phenomenology,'' which has $f_{\eta_{\mathrm{NS}}}=1.07 f_\pi$, $f_{\eta_{\mathrm{S}}}=1.34 f_\pi$, and the mixing angle $\phi=39.3°$ [14,15,18]. ''FKS scheme and theory'' has $f_{\eta_{\mathrm{NS}}}=f_\pi$ as we do, and $f_{\eta_{\mathrm{S}}}=1.41 f_\pi$ and $\phi=42.4°$, very similar to us, and yields curves which we do not plot because they are too close to our predictions.

As stressed by Hayakawa and Kinoshita [27], VMD still provides one of the best fits to the π^0 transition form-factor data. Nevertheless, in contrast to, e.g., compliance of the SD-BS approach with the axial anomaly [28,29], VMD seems to be the ingredient missing in the present approach, which relies on the BC vertex *Ansatz*. Maris and Tandy [30] solved the SD equation for the dressed quark–photon vertex in a model similar to the present one. Their vertex solution exhibits the vector meson pole in the transverse part of the vertex, and this is the chief source of difference from the BC vertex *Ansatz*. Their vertex solution can be reasonably approximated for $Q^2 \geqslant -m_\rho^2$ by a phenomenological vertex *Ansatz*, the longitudinal part of which is given by the BC vertex, while the transverse part contains the ρ-meson pole term contributing significantly for relatively small but nonzero Q^2. The transition form factor was calculated with the VMD-incorporating vertex solution only for π^0 and up to intermediate momenta, the Q^2 range where our curves overshoot. Indeed, the required reduction of $T_{\pi^0}(-Q^2,0)$ was found there [31]. From Eq. (14), it is obvious that this same mechanism would lead, in the low and intermediate Q^2 range, also to the reduction of the η and η' transition form factors considered here.

Finally, in Fig. 1 we also plot some of our model predictions for the Q^2 dependence of the transition form factors when *both* photons are off-shell. In each curve triplet $P=\eta',\eta,\pi^0$, the dashed curve depicts the pertinent transition form factor (13) for the special case of the symmetric $\gamma^*\gamma^*$ virtualities, $Q'^2=Q^2$. Such $\gamma^*\gamma^*$ form factors cannot be compared with experiment at present, since there are no published experimental data for any $\gamma^*\gamma^*\to\pi^0,\eta,\eta'$ transitions yet. Nevertheless, there will hopefully be some such data in the future, from BaBar, Belle, and CLEO [32,33].

The authors acknowledge the support of the Croatian Ministry of Science and Technology Contracts No. 0119261 and No. 009802.

[1] D. Klabučar and D. Kekez, Phys. Rev. D **58**, 096003 (1998).
[2] C. D. Roberts and A. G. Williams, Prog. Part. Nucl. Phys. **33**, 477 (1994).
[3] R. Alkofer and L. von Smekal, Phys. Rep. **353**, 281 (2001).
[4] C. D. Roberts and S. M. Schmidt, Prog. Part. Nucl. Phys. **45**, S1 (2000).
[5] D. Kekez and D. Klabučar, Phys. Lett. B **387**, 14 (1996).
[6] D. Kekez, B. Bistrović, and D. Klabučar, Int. J. Mod. Phys. A **14**, 161 (1999).
[7] D. Kekez and D. Klabučar, Phys. Lett. B **457**, 359 (1999).
[8] D. Klabučar and D. Kekez, Fiz. B **8**, 303 (1999).
[9] H. J. Munczek and P. Jain, Phys. Rev. D **46**, 438 (1992).
[10] P. Jain and H. J. Munczek, Phys. Rev. D **48**, 5403 (1993).
[11] D. Kekez, D. Klabučar, and M. Scadron, J. Phys. G **26**, 1335 (2000).
[12] D. Klabučar, D. Kekez, and M. Scadron, p. 201 in ''Exploring Quark Matter,'' proceedings of the Workshop on Quark Matter in Astro- and Particle Physics, Rostock, Germany, 2000, edited by G. R. G. Burau, D. B. Blaschke, and S. M. Schmidt, hep-ph/0012267.
[13] D. Kekez, D. Klabučar, and M. Scadron, J. Phys. G **27**, 1775 (2001).
[14] Th. Feldmann, P. Kroll, and B. Stech, Phys. Rev. D **58**, 114006 (1998).
[15] Th. Feldmann, P. Kroll, and B. Stech, Phys. Lett. B **449**, 339 (1999).
[16] H. Leutwyler, Nucl. Phys. B (Proc. Suppl.) **64**, 223 (1998).
[17] R. Kaiser and H. Leutwyler, hep-ph/9806336.
[18] See also Table 2 of the review Th. Feldmann, Int. J. Mod. Phys. A **15**, 159 (2000).
[19] CELLO Collaboration, H.-J. Behrend *et al.*, Z. Phys. C **49**, 401 (1991).
[20] R. Alkofer and C. D. Roberts, Phys. Lett. B **369**, 101 (1996).
[21] B. Bistrović and D. Klabučar, Phys. Lett. B **478**, 127 (2000).
[22] J. S. Ball and T.-W. Chiu, Phys. Rev. D **22**, 2542 (1980).
[23] CLEO Collaboration, J. Gronberg *et al.*, Phys. Rev. D **57**, 33 (1998).
[24] L3 Collaboration, M. Acciarri *et al.*, Phys. Lett. B **418**, 399 (1998).
[25] S. J. Brodsky and G. P. Lepage, Phys. Rev. D **24**, 1808 (1981).
[26] Th. Feldmann and P. Kroll, Phys. Rev. D **58**, 057501 (1998).
[27] M. Hayakawa and T. Kinoshita, Phys. Rev. D **57**, 465 (1998).
[28] P. Maris, C. D. Roberts, and P. C. Tandy, Phys. Lett. B **420**, 267 (1998).
[29] P. Maris and C. D. Roberts, Phys. Rev. C **58**, 3659 (1998).
[30] P. Maris and P. C. Tandy, Phys. Rev. C **61**, 045202 (2000).
[31] P. Maris and P. C. Tandy, Nucl. Phys. A **663**, 401 (2000).
[32] V. Savinov, hep-ex/0106013.
[33] M. Diehl, P. Kroll, and C. Vogt, hep-ph/0108220.
[34] Particle Data Group, D. E. Groom *et al.*, Eur. Phys. J. C **15**, 1 (2000).